

LiFePO₄ and graphite electrodes with ionic liquids based on bis(fluorosulfonyl)imide (FSI)[−] for Li-ion batteries

A. Guerfi^a, S. Duchesne^a, Y. Kobayashi^{a,b}, A. Vijn^a, K. Zaghib^{a,*}

^a Institut de Recherche d'Hydro-Québec, Varennes, QC, Canada

^b Central Research Institute of Electric Power Industry, 2-11-1, Iwado Kita, Komae-shi, Tokyo 201-8511 Japan

Received 2 August 2007; received in revised form 4 September 2007; accepted 5 September 2007

Available online 16 September 2007

Abstract

Ambient-temperature ionic liquids (IL) based on bis(fluorosulfonyl)imide (FSI) as anion and 1-ethyl-3-methyleimidazolium (EMI) or *N*-methyl-*N*-propylpyrrolidinium (Py13) as cations have been investigated with natural graphite anode and LiFePO₄ cathode in lithium cells. The electrochemical performance was compared to the conventional solvent EC/DEC with 1 M LiPF₆ or 1 M LiFSI. The ionic liquid showed lower first coulombic efficiency (CE) at 80% compared to EC–DEC at 93%. The impedance spectroscopy measurements showed higher resistance of the diffusion part and it increases in the following order: EC–DEC–LiFSI < EC–DEC–LiPF₆ < Py13(FSI)–LiFSI = MI(FSI)–LiFSI. On the cathode side, the lower reversible capacity at 143 mAh g^{−1} was obtained with Py13(FSI)–LiFSI; however, a comparable reversible capacity was found in EC–DEC and EMI(FSI)–LiFSI. The high viscosity of the ionic liquids suggests that different conditions such as vacuum and 60 °C are needed to improve impregnation of IL in the electrodes. With these conditions, the reversible capacity improved to 160 mAh g^{−1} at *C*/24. The high-rate capability of LiFePO₄ was evaluated in polymer–IL and compared to the pure IL cells. The reversible capacity at *C*/10 decreased from 155 to only 126 mAh g^{−1} when the polymer was present.

© 2007 Published by Elsevier B.V.

Keywords: LiFePO₄; Graphite; Ionic liquid; LiFSI; FSI; Li-ion battery

1. Introduction

Besides the market for portable electronic devices, Li-ion technology is starting to penetrate other markets such as hybrid electric vehicles (HEV) and plug-in HEV (PHEV) [1–4]. However, there are many features that must be resolved before Li-ion batteries are used in HEVs, including low cost, long calendar life, safety and high power capability [5,6]. Safety is one of these crucial issues for advanced applications of Li-ion batteries.

So far, LiCoO₂ has been the main cathode material used in Li-ion batteries, owing to its high energy density. However, the questionable long-term supply of cobalt material and its high cost present an uncertain future. So an alternative cathode material that is Co-free is urgently needed to prepare for the future applications of Li-ion battery technology in HEVs and PHEVs. Since the demonstration of LiFePO₄ by Padhi et al. [7,8] as a

potential cathode material, considerable interest has been generated due to its safety, low cost and environment friendly nature [9–15]. Furthermore, side reactions are minimized because of its flat voltage profile at 3.4 V versus Li/Li⁺. However, some other parts of the battery can cause problems in the scale-up configuration. In Li-ion batteries, we found that in general the nature of electrolyte materials has a great impact on the safety of the battery. In order to improve the safety of lithium batteries, the electrolyte should have lower flammability and lower reactivity than conventional electrolytes. Room-temperature ionic liquids (IL) have suitable properties for use as safe alternative as an electrolyte for lithium batteries due to their non-volatility and inflammability [16].

In this work, we selected 1-ethyl-3-methyleimidazolium (EMI) and *N*-methyl-*N*-propylpyrrolidinium (Py13) as cations and bis(fluorosulfonyl)imide (FSI) for the anion. The ionic liquids were evaluated with graphite anodes and LiFePO₄ cathodes in lithium cells and compared to conventional electrolytes with LiPF₆ or LiFSI salt. The interface impedance, rate performance and cyclability were investigated. Also, we

* Corresponding author. Tel.: +1 450 652 8019; fax: +1 450 652 8424.

E-mail address: zaghib.karim@ireq.ca (K. Zaghib).

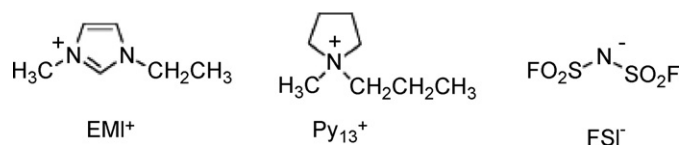


Fig. 1. Chemical structure of ionic liquids used in this study.

examined the performance of Li/LiFePO₄ cells with mixed polymer and ionic liquid in order to understand the role of polymer on the interface stability.

2. Experimental

In this work, we used two ionic liquids; 1-ethyl-3-methylimidazolium-bis(fluorsulfonyl)imide (EMI-FSI), *N*-methyl-*N*-propylpyrrolidinium-bis(fluorsulfonyl)imide (Py13-FSI) based on FSI anion (Fig. 1) obtained from Dai-Ichi Kogyo, Seiyaku Co., Ltd, Japan (DKS). These ILs contain less than 10 ppm (w/w) H₂O, and less than 2 ppm (w/w) of halide and alkali metal-ion impurities. Two organic electrolytes were also evaluated; the standard solvent ethylene carbonate/diethylcarbonate EC/DEC–1 M LiPF₆ (UBE, Japan) was used as the reference. A second organic solvent EC/DEC–1 M LiFSI (HQ, Canada) was used.

A stainless-steel coin cell was assembled with composite electrode containing 5 wt% Poly Vinyl Dene Fluoride (PVDF) (Kureha, Japan), 93% natural graphite (Hydro-Québec) and 2% VGCF (vapour growth carbon fibre, Showa-Denko, Japan) for the anode. The composition of the cathode was 12% PVDF, 82% carbon-coated LiFePO₄ (Phostech-Lithium, Canada), 3 wt% carbon black and 3 wt% VGCF. With the ionic liquid, we added 0.7 M LiFSI in both Py13-FSI and EMI-FSI. The cells contained Celgard (3501), which was soaked in organic solvent or ionic liquid under vacuum at 60 °C. The active surface area is 2 cm². The cell was assembled in a glove box with lithium metal as counter electrode. The electrochemical measurements were performed with a VMP-cycler (Biologic, France). The first formation cycles were realized at constant charge–discharge at *C*/24. The power characteristics of the electrodes were evaluated with the *C*-rate test by varying the discharge current from *C*/12 to 40*C* rate. The conductivity measurements were performed using a model CM-30R conductivity meter (DKK-TOA Corp. Japan). The viscosity was determined using MCR-30 viscometer (Anton-Paar, USA). Owing to its better safety profile, Py13(FSI) was considered for further study in this work.

The effect of vacuum on the performance of the cell was examined with a LiFePO₄ cell. The effect of gel polymer media was investigated with Py13(FSI) ionic liquid. The gel polymer was prepared by mixing 5 wt% polymer based on polyether with four branches (molecular weight 8000, Elexcel 210, DKS, Japan) with Py13(FSI)–0.7 M LiFSI and 1000 ppm of thermal initiator perkadox (Akzo Nobel, USA).

3. Results and their significance

The viscosity and conductivity of the solvent have an inverse relation, thus, electrolytes with lower viscosity are preferred for

Table 1
Viscosity and ionic conductivity of the electrolyte

Electrolyte	Viscosity at 20 °C (mPa s)	Conductivity at 20 °C (mS cm ⁻¹)
EC–DEC (3:7)	7.68 ^a	7.24 ^a
EMI(FSI)	19	17.74
Py13(FSI)	39	9.14

^a Reference [11], data at 25 °C.

use in batteries. The viscosity and conductivity were measured at 20 °C. Table 1 lists the viscosity and ionic conductivity of the pure electrolyte without salt addition. The conventional organic electrolyte has the lowest viscosity, and the ionic liquids with lower viscosity show higher conductivity.

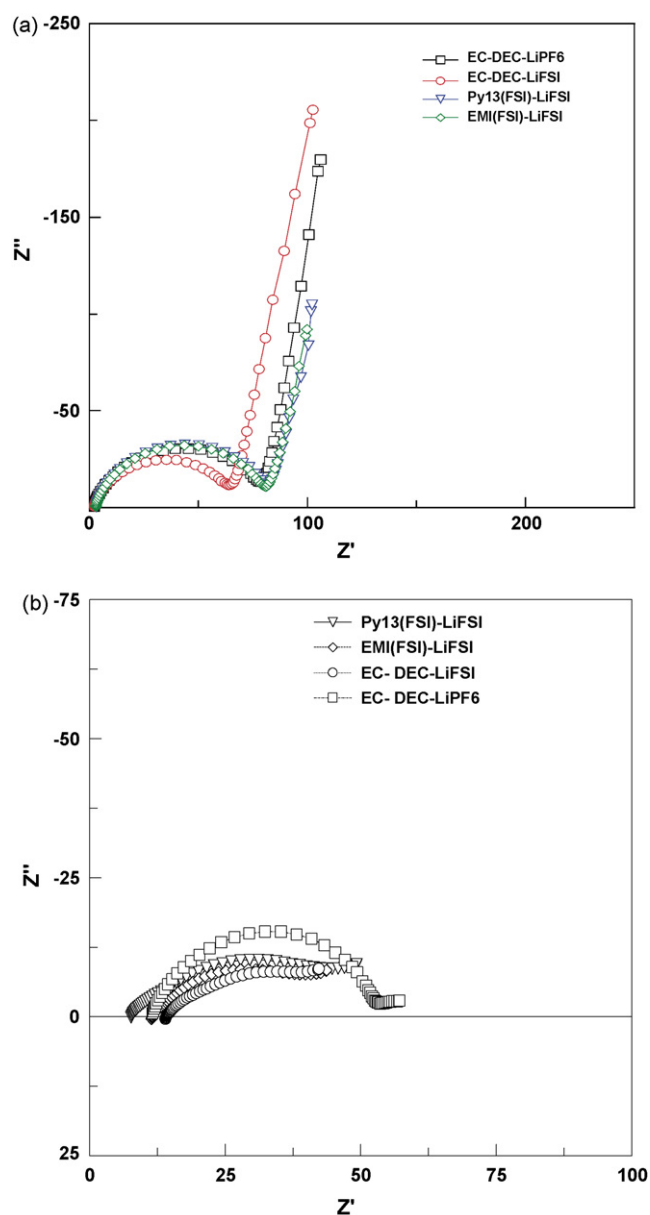


Fig. 2. (a) Impedance spectra of Li/graphite anodes at OCV before SEI formation in different electrolytes. (b) Impedance spectra of Li/graphite anodes at 0 V after SEI formation in different electrolytes.

The conventional electrolyte and ionic liquids cannot be compared with each other because of the different temperatures, different concentrations and the different charge carrier (ions). It is important to emphasize that the inverse correlation between conductivity and viscosity is not just an empirical observation but arises for all liquids including liquid gases, liquid metals, organic liquids, ionic liquids and molten salts, for fundamental theoretical reasons. The Arrhenius type of activation energies for viscous flow, E_n , self-diffusion of cations E_{D+} , and anions E_{D-} , all reveal practically the same value in these liquid systems [17,18]:

$$E_n \approx E_{D+} \approx E_{D-} \approx 3.7RT_m \quad (1)$$

where R is the gas constant and T_m is melting point (in K) of these liquids. Strictly speaking, the ordinary connotation of melting point applies to molten salts and metals, since most gases, organic liquids and ionic liquids are not solid at room temperature; in other words T_m is the temperature of phase change, in Kelvin, that gives rise to the liquid state. Theoretically, Eq. (1) can be interpreted by deducing the heat of activation for transport in liquids in terms of work of hole formation in the liquid, as done by Bockris and coworkers [17–19], following the original formulation of Fürth [20]. Thus, one must seek a liquid (ionic or otherwise) for a battery with the lowest melting point in order to attain the highest conductivity.

3.1. Graphite anode

The impedance measurement at open circuit voltage (OCV) before the formation of the solid electrolyte interface (SEI) is shown in Fig. 2(a); a comparable interface resistance of 80Ω is observed with the ionic liquid and reference electrolyte EC/DEC–LiPF₆ using a graphite anode (versus Li). However, a noticeably lower interface impedance of 65Ω was observed with the electrolyte EC–DEC–LiFSI. In the diffusion part, the ionic liquids show higher resistance and it increases in the following order: EC–DEC–LiFSI <

EC–DEC–LiPF₆ < Py13(FSI)–LiFSI = MI(FSI)–LiFSI = 20Ω . Due to the high viscosity of the IL, the diffusion resistance is consequently higher. The OCV for liquid electrolytes is higher between 3 and 3.1 V, whereas in the case of ionic liquids, the OCV is between 2.8 and 2.9 V. The results of impedance measurements at 0 V (Li_xC₆) after the formation of SEI with two potential cycles are shown in Fig. 2(a); a comparable interface resistance is observed with the ionic liquids and reference electrolyte EC/DEC–LiPF₆ using a graphite anode. This data indicate the SEI layer on graphite is stable in the presence of ionic liquids.

Fig. 3 shows the first two charge–discharge cycles of graphite in EC–DEC–LiPF₆ (a), EC–DEC–LiFSI (b), EMI(FSI) (c) and Py13(FSI) (d). These charge–discharge cycles were obtained at C/24 rate between 0 and 2.5 V at ambient temperature.

For the standard cell (a), a reversible capacity of 365 mAh g^{-1} was obtained at the second discharge that is very close to the theoretical capacity (372 mAh g^{-1}). Furthermore, a high coulombic efficiency in the first cycle (CE1) of 92.7% was observed; these data reflect the performance of our electrodes in the standard electrolyte that will be used as reference for comparison in this study.

When LiPF₆ is replaced by LiFSI salt (b), the anode shows excellent performance in the first cycle, with a reversible capacity (369 mAh g^{-1}) close to the theoretical capacity, and a coulombic efficiency of 93%. The LiFSI salt has a positive effect on the formation of coherent passive layer on the graphite.

In Fig. 3, the cell with IL based on EMI-FSI (c) showed a reversible capacity of 362 mAh g^{-1} , but the coulombic efficiency was only 80.5%. However, with the ionic liquid Py13 (d), the reversible capacity of 367 mAh g^{-1} is also close to the theoretical capacity, and the first coulombic efficiency of 80% is the same as that obtained with the other IL used in the study. These results indicate that LiFSI salt in FSI based ionic liquid is suitable for use with graphite side, where any secondary reaction is minimal.

In Table 2, we summarize some of the electrochemical data for the graphite anode in standard electrolyte and ionic liquid

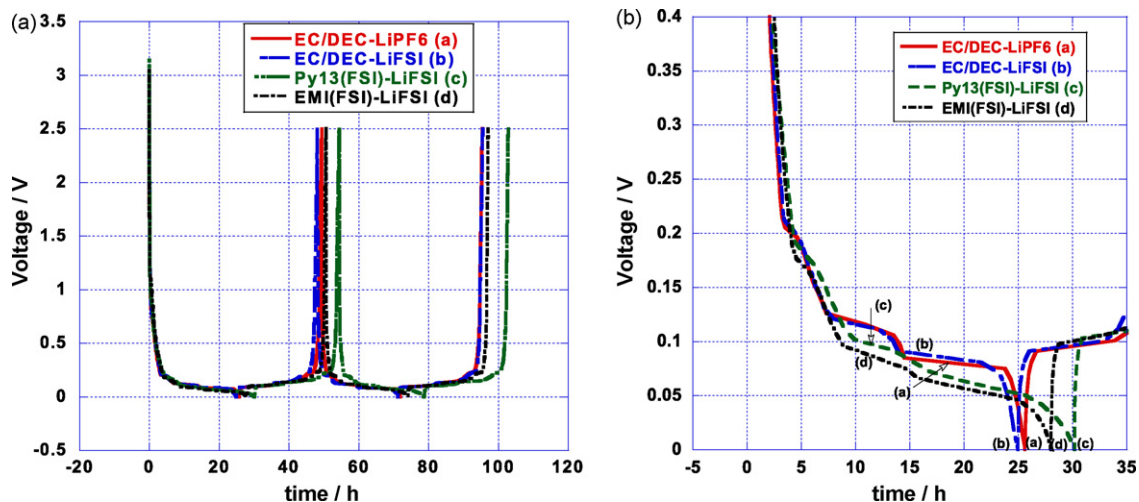


Fig. 3. First two charge–discharge cycles for Li/graphite anodes in different electrolytes (a). An expanded profile of the first cycle between 0.5 and 0 V is also presented (b).

Table 2

Electrochemical characteristics of the graphite anode in the first two charge–discharge cycles

Electrolyte	1st discharge (mAh g ⁻¹)	CE1 (%)	Reversible capacity (mAh g ⁻¹)	CE2 (%)
EC–DEC–1 M LiPF ₆	398	92.7	365	100
EC–DEC–1 M LiFSI	382	9.0	369	100
Py13(FSI)+0.7 M LiFSI	468	80	367	98.3
EMI(FSI)+0.7 M LiFSI	432	80.5	362	97.6

electrolyte. The coulombic efficiency in the second cycle (CE2) with IL still does not reach 100%, which probably is due to some side reactions, and the passivation layer on graphite cannot be established during the first cycles (Fig. 3b).

The cyclability of the cells was evaluated at 1C in discharge and C/4 for charging. The discharge capacities of the graphite with various electrolytes are shown in Fig. 4. The capacity was quite stable for the organic electrolyte during the first 10 cycles, with a slightly lower reversible discharge capacity in LiPF₆ compared to LiFSI salt. On the other hand, when the electrolyte is an ionic liquid, the discharge capacity still increased during the first five cycles for Py13(FSI) and 10 cycles for EMI(FSI). This result suggests that the IL electrolyte, Py13(FSI), probably requires more cycles than the standard electrolytes to form a stable passivation layer on the graphite surface particles. For the IL electrolyte, EMI(FSI), the capacity increases can be attributed to the improved wettability in the electrode upon repetitive lithium intercalation/deintercalation in graphite. However, Ishikawa [21] reported quite stable cyclability of the Li/graphite anode in ionic liquid EMI(FSI) with 0.8 M LiTFSI salt, and they show a stable capacity of 360 mAh g⁻¹ at C/5. These data suggest that the combined stabilizing effect of FSI cation in IL, and

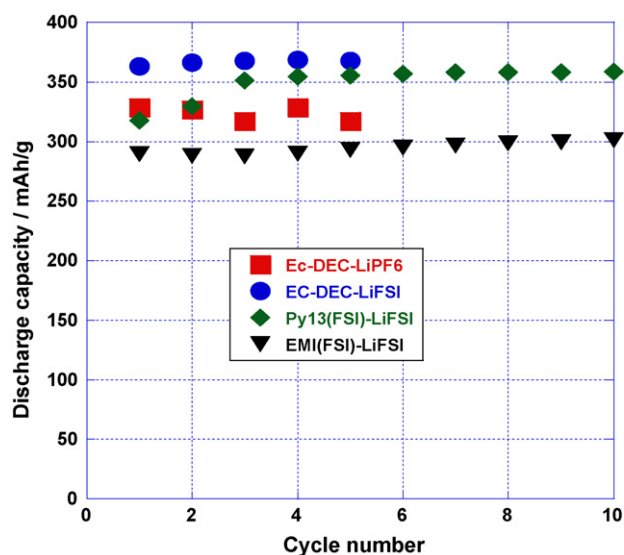


Fig. 4. Cycling behaviour of Li/graphite anodes in different electrolytes represented as discharged capacity (mAh g⁻¹).

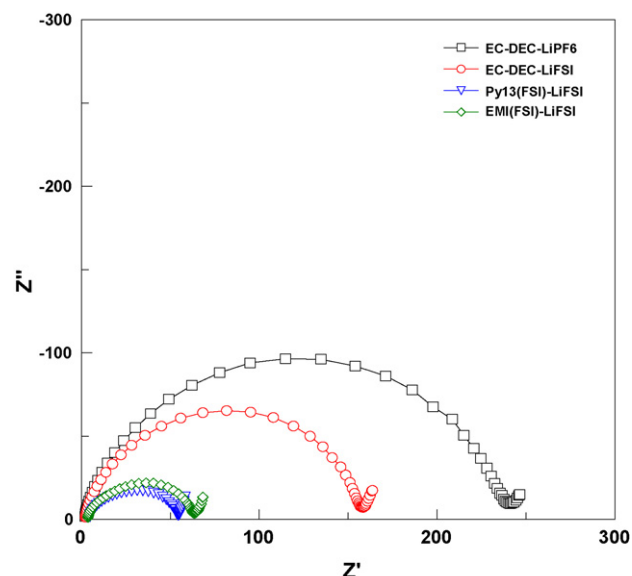


Fig. 5. Impedance profiles of Li/LiFePO₄ cathodes in different electrolytes.

the effect of the Li salt on the SEI layer on graphite, play a role in achieving high reversible capacity.

3.2. LiFePO₄ cathode

The impedance at OCV of cells with LiFePO₄ cathodes and different electrolytes (i.e., organic and ionic liquids) was determined by impedance spectroscopy. The impedance profiles (Fig. 5) show that the interfacial resistance of cells with a LiFePO₄ cathode was very different from that observed in cells with graphite anodes (Fig. 2). The highest interface resistance with a reference electrolyte (EC–DEC–1 M LiPF₆) was 240 Ω. The ionic liquids both showed lower interface resistance—54 and 64 Ω for Py13(FSI) and EMI(FSI), respectively. One possible explanation for this result is that the cathode was not completely wetted by the ionic liquid in the cell when the electrode was simply dipped in IL under normal condition. Perhaps, some of the LiFePO₄ particles did not have a passivation layer yet, and thus, did not contribute to the total resistance of the cathode interface.

The electrochemical performance of the Li/LiFePO₄ cells was examined with ionic liquids and compared to the performance in the conventional organic solvent. Fig. 6 shows the first charge–discharge curves at C/24 between 4 and 2.5 V. The reversible capacity and the coulombic efficiency are summarized in Table 3. The reversible capacity with EC–DEC–LiPF₆

Table 3

Electrochemical characteristics of the LiFePO₄ cathode in different electrolytes

Electrolyte	1st discharge (mAh g ⁻¹)	CE1 (%)	Reversible capacity (mAh g ⁻¹)	CE2 (%)
EC–DEC–1 M LiPF ₆	158	98	158	98
EC–DEC–1 M LiFSI	157	98	157	98
Py13(FSI)+0.7 M LiFSI	151	93	143	98
EMI(FSI)+0.7 M LiFSI	164	95	160	97

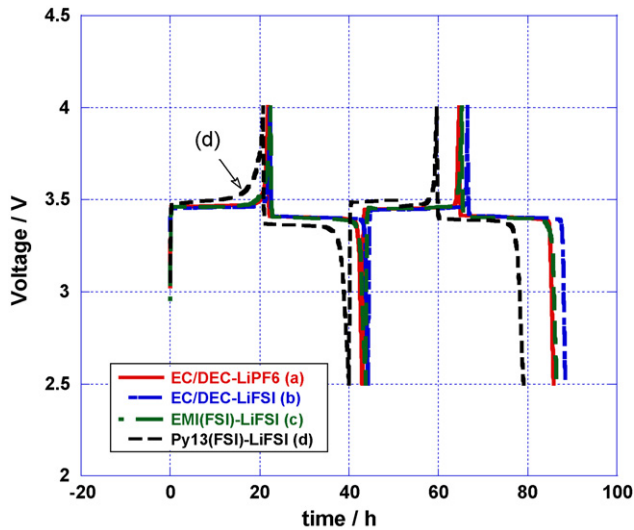


Fig. 6. The first charge–discharge cycle of Li/LiFePO₄ cells in different electrolytes.

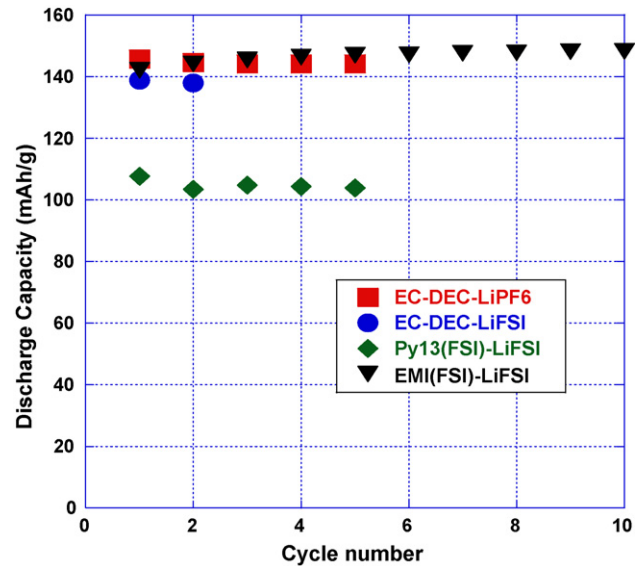


Fig. 7. Cycling behaviour of Li/LiFePO₄ cells in different electrolytes.

(a) was 158 mAh g⁻¹ and 98% coulombic efficiency in the first cycle (CE1). The charge–discharge result with LiFSI salt (b), the reversible capacity (157 mAh g⁻¹) was similar to that with EC–DEC–LiPF₆ electrolyte, and the first cycle coulombic efficiency (98%) was also the same. With the ionic liquid Py13(FSI) (c), a lower reversible capacity (143 mAh g⁻¹) was obtained, and the coulombic efficiency (93%) was also lower. However, with ionic liquid EMI(FSI), indicated by curve (d), a much higher reversible capacity (160 mAh g⁻¹) and modest improvement in coulombic efficiency (95%) were obtained.

The high viscosity of Py13(FSI), two times that of EMI(FSI), can make the lithium extraction from LiFePO₄ structure more difficult even at low rate like C/24. This result is clearly described on the charge curve with not well-defined curvature at the end of the charging plateau.

In the cells containing LiFePO₄, the electrolyte viscosity may affect the performance due to the carbon coating on the surface of the LiFePO₄ particles. When the electrolyte has high viscosity, like an ionic liquid, the wettability of the carbon layer is more difficult. In this case, lithium ions are not able to easily migrate to the carbon layer and through it, particularly in the first cycles. Moreover, high viscosity can mitigate also the uniform wettability of the electrodes in depth, both anode and cathode, because of the quasi three-dimensional fractal nature of the electrodes.

The cycling data at 1C rate on discharge and C/4 rate on charge are presented in Fig. 7. The highest capacity (145 mAh g⁻¹) was obtained with EMI(FSI), whereas the results with EC–DEC–LiPF₆ and EC–DEC–LiFSI were both lower, 137 and 139 mAh g⁻¹, respectively. However, Py13(FSI) showed a lower initial capacity that decreased to 105 mAh g⁻¹ in five cycles. The coulombic efficiency for all the electrolytes stabilized at 100% in the second cycle, except for the Py13(FSI), for which the coulombic efficiency reaches 100% only in the 6th cycle. Since ionic conductivity is inversely related to viscosity, the Py13(FSI) electrolyte does not as easily wet the electrodes;

the tendency is for a lower capacity at 1C compared to other electrolytes.

In order to investigate the power performance of LiFePO₄ in different electrolytes, a rate-capability test was applied in which increasing discharge rates were used. The rate dependence of the different electrolytes is summarized in Fig. 8. The discharge current was varied at different rates while the charge current was maintained constant at C/4. The electrolyte EC–DEC–LiFSI shows a reasonable performance at high rate, for example, at 15C rate, high discharge capacities were delivered by the cell having LiFSI with 105 mAh g⁻¹. For rates above 20C, the capacity starts diverging from the cell having LiPF₆ as salt. With the ionic liquid of higher viscosity, EMI(FSI), comparable performance was obtained up to the 1C rate, but at rates over 4C, the capacity dropped to 45 mAh g⁻¹ and lower. For a more viscous electrolyte such as Py13(FSI), the C-rate performance was lower and the divergence to the rate capability of other cells starts at C/2 rate. At 4C, the capacity dropped to a low value of 40 mAh g⁻¹.

From these data, it is clear that the power performance is strongly dependent on the viscosity and ionic conductivity

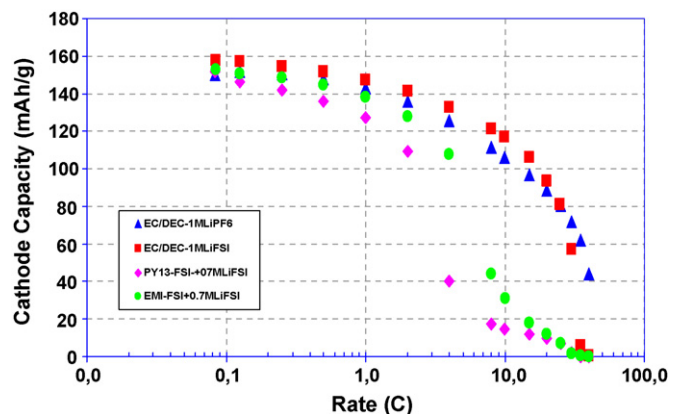


Fig. 8. Rate capability of Li/LiFePO₄ cells at different discharge rate in different electrolytes.

of the electrolyte. Furthermore, the electrolytes with both organic and ionic liquids and LiFSI salt showed good results. Matsumoto et al. [22] compared the high-rate performance of Li/LiXX-EMI/LiCoO₂ cells (XX = FSI or TFSI anion). He confirmed the higher performance of EMI when FSI anion is used. He also observed that the capacity retention ratio 1/0.1C for EMI(FSI) and Py13 (FSI) cells was 93 and 87%, respectively. However, when TFSI anion is used, the EMI(TFSI) cell has a much lower capacity retention ratio 1/0.1C of only 43%. Furthermore, the performance of these ionic liquids not only depends on the viscosity and conductivity but also on the anion and on the Li salt.

In further tests, we selected Py13(FSI) IL, because of its higher safety level as reported by Dahn et al. [23]. In order to improve the wettability of cathodes with the ionic liquid, LiFePO₄ was pre-treated by immersing it in Py13(FSI)-LiFSI IL, followed by putting it under vacuum at 60 °C for 8 h. This cathode was then evaluated in a lithium metal cell. The first charge–discharge cycles of the pre-treated cell at 25 °C are shown in Fig. 9, compared to a cell at 25 °C that was prepared without vacuum. The coulombic efficiency improved in the first and second cycles to 100% compared to 93% and 98% due to the beneficial effect of the vacuum pre-treatment and enhanced wettability. The impedance spectra of these cells before and after cycling are shown in Fig. 10. The interfacial resistance is initially higher when the cathode is pre-treated under vacuum—70 Ω versus 50 Ω. However, after two cycles at C/24, the interface impedance of the pre-treated cathodes decreases. The reversible capacity was increased by 14% to 160 mAh g⁻¹. The cycling life at 1C shows stable capacity at 140 mAh g⁻¹, with an improvement of 36% (Fig. 11). The viscosity of IL Py13(FSI) was about two times that of EMI(FSI) (Table 1).

The high-rate capability shows a small increase in the power performance in the range above about 2C rate (Fig. 12). However, for the higher rates, the capacity dropped comparably to the same level as in cells in which cathode wetting was not improved

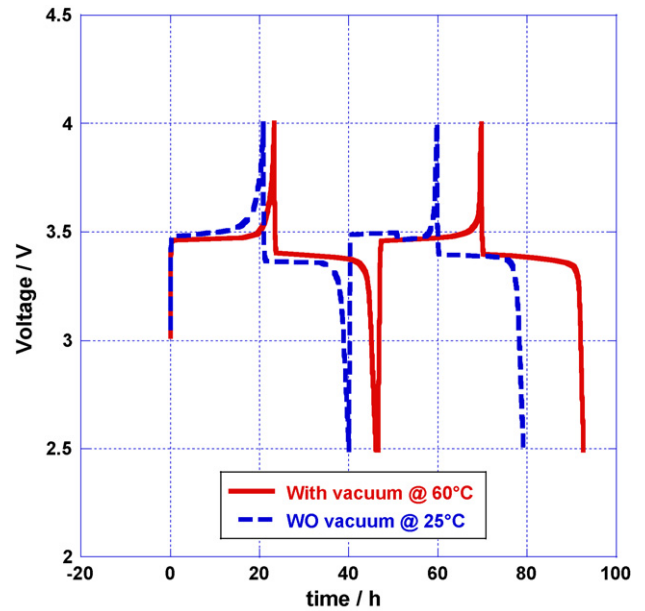


Fig. 9. The first charge–discharge cycle of Li/LiFePO₄ cells with Py13(FSI)-LiFSI, with and without vacuum.

with vacuum pre-treatment, as described above. At below 2C rate, a large increase in the capacity from 40 to 80 mAh g⁻¹ is observed.

3.3. Ionic liquid–polymer

The gel–polymer media was considered in this study as a potential electrolyte having zero vapour pressure. The cell LiFePO₄/Py13(FSI)-LiFSI-polymer/Li was evaluated to improve cell safety. Due to the high viscosity of the polymer/Py13(FSI)-LiFSI solution, the cathode was prepared under vacuum at 60 °C for 5 h. High interfacial resistance (220 Ω) was observed with polymer cell, which dropped to 140 Ω after two

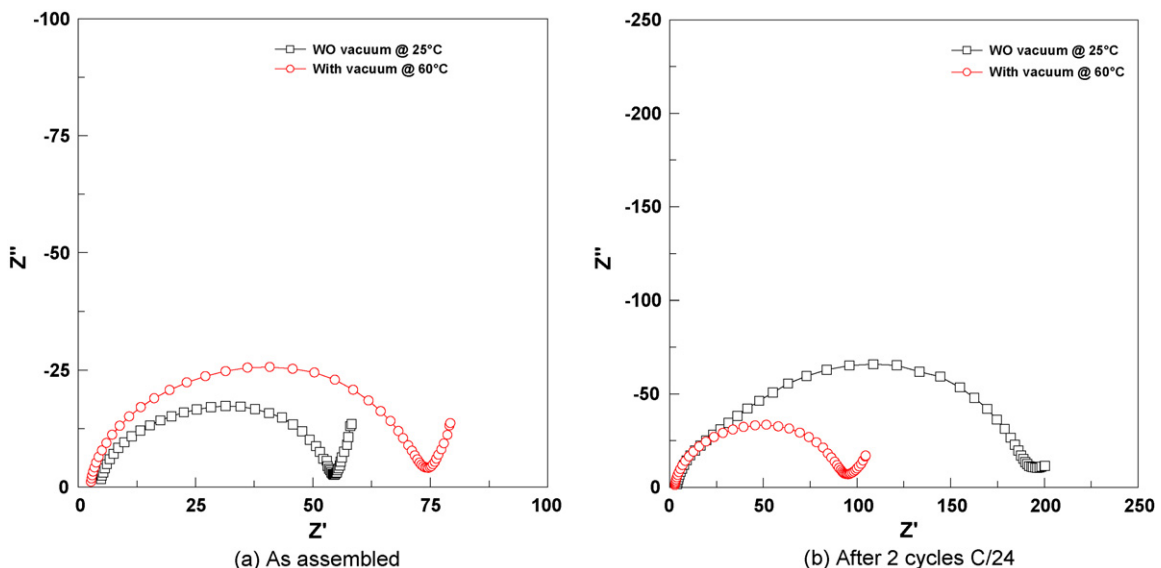


Fig. 10. Impedance of Li/LiFePO₄ cells with Py13(FSI)-LiFSI, (a) freshly-assembled cells, and (b) after two cycles.

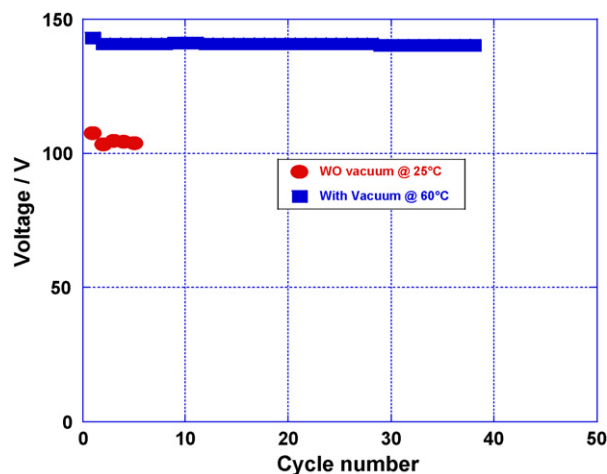


Fig. 11. Cycling behaviour of Li/LiFePO₄ cells with Py13(FSI)-LiFSI, with and without vacuum pre-treatment.

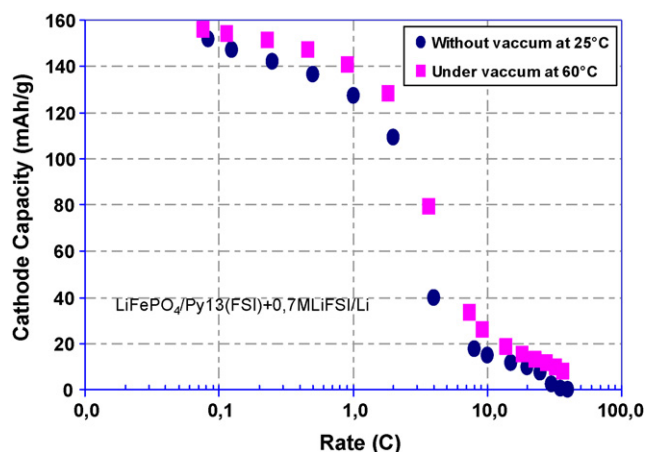


Fig. 12. Rate capability of Li/LiFePO₄ cells with Py13(FSI)-LiFSI, with and without vacuum pre-treatment.

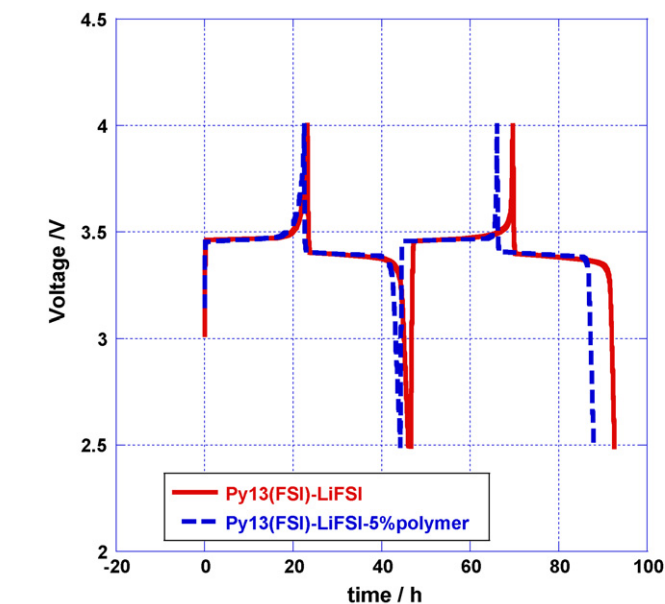
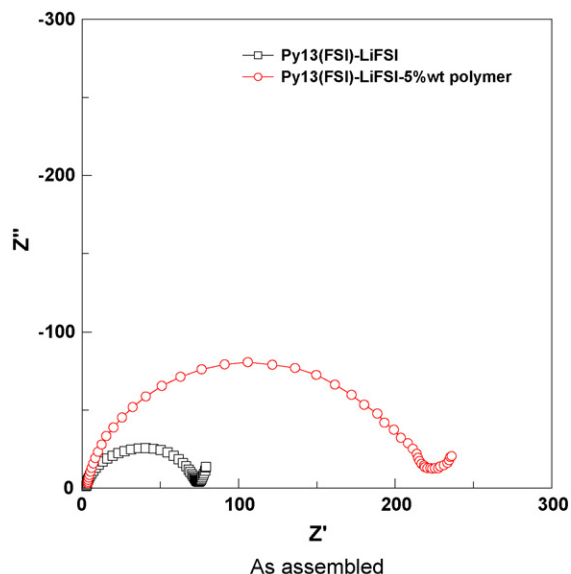


Fig. 14. The first charge-discharge of Li/LiFePO₄ cells with Py13(FSI)-LiFSI + 5% polymer compared to IL alone.

cycles at $C/24$. Contrary to the ionic liquid case, the interfacial resistance increased after two cycles at $C/24$ (Fig. 13). From these data, we speculate that, the IL forms a thin passive layer, but it keeps growing even after cycling. When polymer is added (5 wt%), the interfacial resistance increases due to the resistivity of the polymer at 25 °C, but with further cycling, passivation becomes pronounced and stabilizes, which is not the case with IL alone.

The electrochemical performance at low rate of the ionic liquid with and without polymer is presented in Fig. 14. The coulombic efficiencies are 93 and 98%, respectively, for the first and second cycles. The reversible capacity was only 141 mAh g⁻¹. The power decreases when polymer is

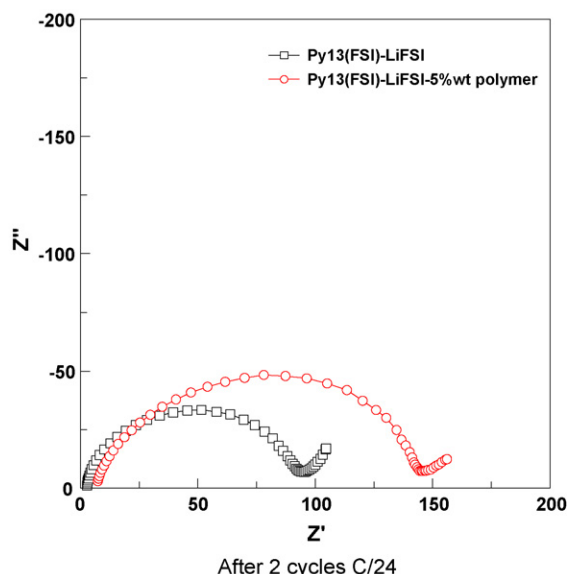


Fig. 13. Impedance profiles of Li/LiFePO₄ cells with Py13(FSI)-LiFSI + 5% polymer as gel electrolyte compared to IL alone.

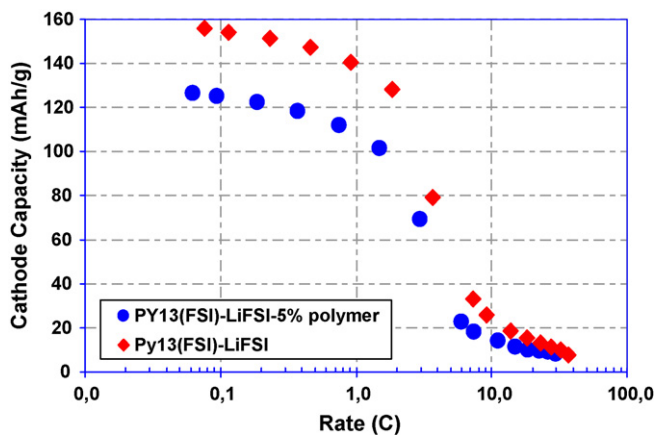


Fig. 15. Rate capability of Li/LiFePO₄ cells with Py13(FSI)–LiFSI + 5% polymer compared to IL alone.

added. At $C/10$, only 126 mAh g^{-1} was delivered compared to 155 mAh g^{-1} . At $1C$ rate, the capacity was 106 mAh g^{-1} compared to 140 mAh g^{-1} ; however, at $10C$ rate, the capacity is comparable (Fig. 15).

The main significance of the results is that IL-based electrolytes are capable of offering performance comparable to the conventional liquid electrolyte. Thus, there are opportunities for developing safer Li-ion batteries containing electrolytes with low vapour pressure and lower resistance. Chemical stability to oxidation and other reactions that present safety hazards must also be considered. Also, when such an electrolyte is combined with LiFePO₄ cathodes, one reduces the issues of cost, uncertain availability and environmental concern with LiCoO₂.

4. Conclusion

The high viscosity of ionic liquids demands that different pre-treatments such as vacuum and 60°C are required to improve impregnation of IL in the electrode. The SEI layer on graphite in IL was very stable after the first cycle, which yielded 80% coulombic efficiency. The reversible capacity was stable at $1C$ cycling, and the highest value, 360 mAh g^{-1} , was obtained with Py13(FSI). The FSI salt in EC/DEC produced a stable SEI with good reversible capacity of 369 mAh g^{-1} at $1C$ rate, close to the theoretical value.

With regard to the type of cathode, the reversible capacity improved to 140 mAh g^{-1} at $1C$ for Py13(FSI) by using a vacuum pre-treatment. The EMI(FSI) IL shows the highest capacity, 148 mAh g^{-1} , even higher than that obtained with the reference electrolyte.

In this study, we confirmed that electrolytes containing the LiFSI salt yield good performance in our cell tests. Also, the ionic liquid with FSI as counter anion is a good candidate for use in Li-ion batteries. However, for large Li-ion batteries in transportation applications, the safety aspect is the highest priority in selection of the electrode and electrolyte compositions.

With this in mind, graphite/Py13(FSI)–LiFSI/LiFePO₄ seems to be the best choice in terms of safety and reversible capacity of the anode and cathode. However, the power performance is limited to $4C$ rate, that indicates further improvement is needed. The addition of a polymer to the ionic liquid improves the stability of the passivation layer; however, with 5 wt% polymer the interfacial impedance is higher than with IL alone. More work is needed to understand, more fully, the effect of polymer addition in the IL on the interfacial properties and electrochemical performance, free of liquid vapour pressure in the battery.

Acknowledgments

The authors would like to acknowledge the support of the U.S. Department of Energy under the BATT program (Lawrence Berkeley National Laboratory), Central Research Institute of Electric Power Industry and Hydro Québec.

References

- [1] T. Tanaka, K. Ohta, N. Arai, *J. Power Sources* 97–98 (2001) 2.
- [2] R.A. March, S. Vukson, S. Sarampudi, B.V. Ratnakumar, M.C. Smart, M. Manzo, P.J. Dalton, *J. Power Sources* 97–98 (2001) 236.
- [3] T. Takamura, *Solid State Ionics* 152–153 (2002) 19.
- [4] K. Zaghbi, P. Charest, A. Guerfi, J. Shim, M. Perrier, K. Striebel, *J. Power Sources* 134 (2004) 124.
- [5] PNGV FreedomCar manual, T.Q. Duong, *J. Power Sources* 89 (2000) 244.
- [6] N. Terada, T. Yanagi, S. Arai, M. Yoshikawa, K. Ohta, N. Nakajima, N. Arai, *J. Power Sources* 100 (2001) 80–92.
- [7] A.K. Padhi, K.S. Nanjundaswamy, J.B. Goodenough, *J. Electrochem. Soc.* 144 (1997) 1188.
- [8] A.K. Padhi, K.S. Nanjundaswamy, C. Masquelier, S. Okada, J.B. Goodenough, *J. Electrochem. Soc.* 144 (1997) 1609.
- [9] K. Striebel, A. Guerfi, J. Shim, M. Armand, M. Gauthier, K. Zaghbi, *J. Power Sources* 119–121 (2003) 951.
- [10] T. Nakamura, Y. Miwa, M. Tabuchi, Y. Yamada, *J. Electrochem. Soc.* 153 (2006) A1108.
- [11] D.Y.W. Yu, K. Donoue, T. Inoue, M. Fujimoto, S. Fujitani, *J. Electrochem. Soc.* 153 (2006) A835.
- [12] K. Zaghbi, K. Striebel, A. Guerfi, J. Shim, M. Armand, M. Gauthier, *Electrochim. Acta* 50 (2004) 263.
- [13] M. Takahashi, H. Ohtsuka, K. Akuto, Y. Sakurai, *J. Electrochem. Soc.* 152 (2005) A899.
- [14] K. Striebel, J. Shim, V. Strinivasan, J. Newman, *J. Electrochem. Soc.* 152 (2005) A664.
- [15] K. Zaghbi, C.M. Julien, *J. Power Sources* 142 (2005) 279.
- [16] H. Sakaebe, H. Matsumoto, in: H. Ohno (Ed.), *Electrochemical Aspects of Ionic Liquids*, John Wiley and Sons, Inc., Hoboken, NJ, 2005, pp. 173–186.
- [17] L. Nani, J.O'M. Bockris, *J. Phys. Chem.* 67 (1963) 2865.
- [18] J.O'M. Bockris, S.R. Richards, *J. Phys. Chem.* 69 (1965) 671.
- [19] T. Emi, J.O'M. Bockris, *J. Phys. Chem.* 74 (1970) 159.
- [20] R. Fürth, *Proc. Camb. Philos. Soc.* 37 (1941) 252.
- [21] M. Ishikawa, T. Sugimoto, M. Kikuta, E. Ishiko, M. Kono, *J. Power Sources* 162 (2006) 658.
- [22] H. Matsumoto, H. Sakaebe, K. Tatsumi, M. Kikuta, E. Ishiko, M. Kono, *J. Power Sources* 160 (2006) 1308.
- [23] Y. Wang, K. Zaghbi, A. Guerfi, F.F.C. Bazito, R.M. Torresi, J.R. Dahn, *Electrochim. Acta* 52 (2007) 6346.